Modified Poly (Styrene Maleic Anhydride) Copolymer for the Removal of Toxic Metal Cations from Aqueous Solutions

Eman Abo-Baker[2], Said S. Elkholy[1], Maher Z. Elsabee[1,*]

[1]Department of Chemistry, Faculty of science, Cairo University, Egypt
[2]Polymers and Pigments Dept., National Research Center, Dokki, Cairo, Egypt

Abstract   Poly (styrene-maleic anhydride) (SMA) copolymer was modified by reacting the anhydride group with two diamines derivatives. The modified copolymers were characterized by spectral, thermal and X-ray analyses. The obtained product was used for Cd (II), Cu (II) and Pb (II) uptake from aqueous solutions. The absorption process was followed using atomic absorption spectrometry. The effects of several experimental parameters such as pH, concentration and adsorption time on the extent of cations absorption were studied. The equilibrium removal performance of the copolymer is analyzed according to the Langmuir and Freundlich adsorption isotherm model that shows result fitted to both models. Some kinetic models were applied to fit the absorption mechanism.

Keywords   Styrene maleic anhydride copolymer, Diamine, Adsorption isotherms, Metal uptake

1. Introduction

Contamination of aqueous environments by heavy metals and dyes is a worldwide environmental problem because these substances are not biodegradable and are highly toxic to living organisms. Toxic metals such as Cu, Cd, and Pb have become an eco-toxicological hazard of prime interest and increasing significance owing to their tendency to accumulate in the vital organs in humans, animals and accumulation through the food chain [1–3]. Copper pollution arises from copper mining and smelting, brass manufacture, electroplating industries and excessive use of Cu-based agri-chemicals. Copper along with arsenic and mercury, is recognized as the highest relative mammalian toxic [4] and continued inhalation of copper containing sprays is linked with an increase in lung cancer among exposed workers [5].

Cadmium is introduced into water bodies from smelting, metal plating, cadmium–nickel batteries, phosphate fertilizers, mining, pigments, stabilizers, alloy industries and sewage sludge. The harmful effects of cadmium include number of acute and chronic disorders such as "itai–itai" disease, renal damage, emphysema, hypertension and testicular atrophy [6]. Lead is neurotoxic and children are particularly vulnerable because of the rapidly developing nervous system. Lead is known to inhibit the activity of three critical enzymes (5-aminolaevulinate dehyratase (ALA-D), coproporphyrinogen oxidase (COPRO-O) and ferrochelatase (FERRO-C)) critical in heme synthesis, causing abnormal concentrations of heme precursors in blood and urine [7]. Lead (Pb) is discharged into the environment from automobile exhausts, industrial sources. In the soil, Pb is converted to forms unavailable to plants. Any lead that is absorbed by plants tends to remain in the roots and is not transported to the shoots [7]. Hence, removal of copper, cadmium and lead from water and wastewater assumes importance.

There are several methods to treat the metal contaminated effluent such as precipitation, ion exchange and adsorption, etc. [8, 9]. Among all the approaches proposed, adsorption is one of the most popular methods and is currently considered as an effective, efficient and economic method for wastewater purification [10,11]. Presently low cost adsorbents are becoming the focus of many investigations on the removal of heavy metals from aqueous solutions. Removal of copper and cadmium from the aqueous solutions was also achieved by activated carbon.

In this regard, synthesis of new adsorbents from a variety of low‑cost synthetic polymers using chelate-forming polymeric ligands is noteworthy [11, 12].

Styrene-maleic anhydride copolymer (SMA) is a well-known commercialized polymer [13] that has attracted special attention due to the advantage of its convenient preparation [14] and solubility of alkali salt in water, as well as it is a spaghetti-shaped linear polymer with varying lengths (that is to say that the distribution of relative

molecular mass can be adjusted) [15]. The presence of maleic anhydride (MA) moiety along its backbone structure improves its absorption capacity especially after the hydrolysis of the maleic anhydride moiety into carboxylic acid group with increasing hydrophilicity of the polymer [16]. The copolymerization of MA with vinyl monomers and their subsequent hydrolysis have also led to copolymers exhibiting remarkable selectivity toward divalent metal-ion uptake [17-19].

In this work, we reveal a new reactive copolymer that has been prepared by the modification of SMA copolymer by diamines. The presence of carboxylic groups in the same polymer with diamine groups should provide the polymer with the high hydrophilicity required for the fast kinetics of metal uptake.

2. Experimental

2.1. Materials

Ethylene diamine and hexamethylene diamine are products of Aldrich. Styrene/maleic anhydride (SMA-40 XIRAN®), (Molecular Weight Mw, 6094 g/mole and Resin Molecular Weight, Mn 3500 g/mole GPC) were kindly supplied by Polyscope Polymers Company, Netherlands. Tetrahydrofuran (THF), ethanol and diethyl ether from the local market were used as received.

2.2. Preparation of SMA-Diamine Derivative

A solution of SMA in (THF) was added to diamine derivatives. A twofold excess of diamines to SMA was employed to avoid the possible cross linking side reaction between the SMA and diamines [19, 20]. A molar ratio of the anhydride unit, diamine derivatives of 1:2 was used. The mixture was stirred for 6 h, and finally precipitated into (THF) followed by the removal of THF. The precipitate was washed with ethanol several times and re-precipitated in diethyl ether. The products obtained are Styrene maleic anhydride ethylene diamine SMA-EthDA and Styrene maleic anhydride hexamethylene diamine SMA-HmDA. Scheme 1 describes the preparation process.

n=1
=3
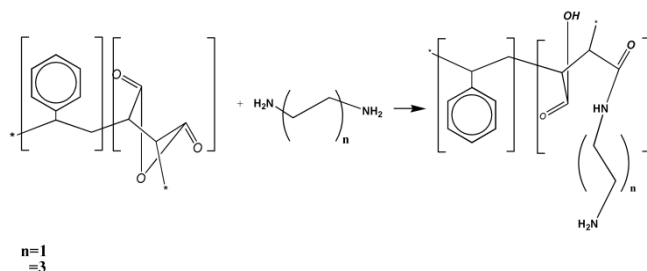
Scheme 1. SMA and diamine derivative

2.3. Characterizations

FTIR infrared measurement was obtained using a Perkin–Elmer 398 FTIR spectrophotometer between 400 and 4000 cm^{-1}. Thermogravimetric analysis TGA studies were performed on a Shimadzu TGA-50H instrument. The samples were heated at a rate of 10°C/min in nitrogen atmosphere.

2.4. pH Study of Adsorption onto the Modified SMA Copolymer

The experiments performed to determine the effect of pH on Cd (II), Cu (II) and Pb (II) adsorption were carried out by placing 0.1 g of the dry copolymer in series of flasks containing 20 ml 500 mg/L metal ion solution. The desired pH was adjusted using 0.1M HCl and 0.1M NaOH. The flasks were shaken for 24 h at 25°C. After adsorption, the filtrate of each flask was analyzed for the metal ion concentration by Atomic Absorption Spectrometer.

2.5. Adsorption Kinetics

Copper (II), cadmium (II) and lead (II) solutions with the desired concentration (1000 mg/L) were prepared from copper (II) chloride anhydrate, cadmium chloride and lead chloride in deionized water. Approximately (0.05) g of tested copolymer were added to a 20 ml of stock solution. The flasks were sealed and shaken at 150 rpm in a constant temperature shaker at 25°C, and were then taken out at a desired time interval. Finally, the concentration of copper, cadmium and lead in each solution were determined using a Varian Spectr AA 220FS atomic adsorption spectrometer.

The adsorbed amounts of copper, cadmium and lead per weight of samples at time t, $q_t = (mg.g^{-1})$, were calculated from the mass balance equation as [21]

$$q_t = \frac{(C_o - C_t)V}{m} \qquad (1)$$

Where Co (mg.L^{-1}) and Ct (mg.L^{-1}) represent the initial and the concentrations of Cu, Cd and Pb at a given time t (min), respectively, V (ml) is the volume of the solution and m (g) is the weight of modified SMA polymer in the flask.

2.6. Adsorption Isotherms

0.1 g dry copolymer was placed in a flask then 20 ml of metal ion solution at a given concentration was added, and the pH value was recorded. The flasks were shaken at 150 rpm for 24 h while keeping the temperature at 25°C. The concentration of the solution was determined by Atomic Adsorption spectrometer and the metal ion uptake q_∞ (maximum amount adsorbed) was calculated using the following equation:

$$q_\infty = \frac{v}{m}(C_o - C_\infty) \qquad (2)$$

2.7. X-ray Diffraction

X-ray diffraction analysis (XRD) was carried out by a Scintag powder diffractometer. The X-ray diffraction patterns were determined in powdery samples with Ni-filtered CuKα at 40 kV and 40mA were recorded from angles of 5.00–90.00° in 2θ.

3. Results and Discussion

3.1. Characterization

3.1.1. Elemental Analysis

The elemental analysis results of copolymers are shown in Table (1). The nitrogen content (7-9%) in** the two modified copolymers reveals that the reaction between SMA and diamine derivatives has occurred.

Table 1. Elemental analysis data for SMA and SMA di-amine derivatives

Composition	C%	H%	N%
SMA	69.98	3.66	0.00
SMA- EthDA	58.36	7.93	9.13
SMA- HmDA	61.88	9.16	7.45

3.1.2. Infrared Spectra Analysis

FTIR spectroscopy has been used for the characterization of the SMA copolymer and the modified SMA copolymer

As shown in Figure. (1) the presence of some hydrolyzed carboxylic groups which can be identified by the presence of a broad pronounced band at around 3443 cm^{-1}. The band at 2940 cm^{-1} is due to the C-H stretching in the backbone of the SMA copolymer. The prominent absorption bands in the ranges of 1840–1887 and 1778 – 1725 cm^{-1} are assigned to the asymmetrical and symmetrical stretching vibration of C=O groups of the maleic anhydride moieties in the copolymer, respectively. The absorptions at 3500–3000 cm^{-1} and 1630–1640 cm^{-1} indicate the presence of aromatic ring. After the reaction, a decrease in the intensity of the MA absorption with the appearance of new peak at 1500 cm^{-1} was observed. In the fingerprint region, the peak at 1555-1557 cm^{-1} is attributed to the stretching of the grafted diamine.
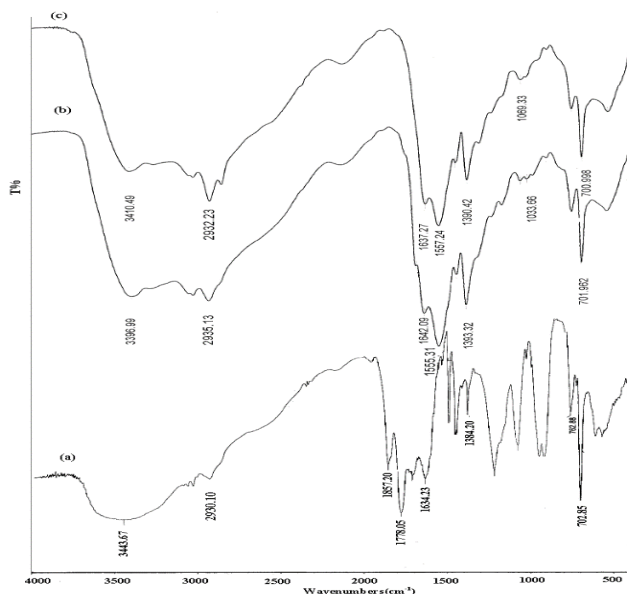

Figure 1.　(a) SMA, (b) SMA-EthDA, (c) SMA-HmDA

The peak intensity at 2870 cm^{-1} (CH$_3$ stretch) and 2930 cm^{-1} (CH$_2$ stretch) become stronger due to the ethylene and hexamethylene diamine contribution. The absorption peak at 1600 cm^{-1} may be attributed to the carbonyl group of the amide-acid.

3.1.3. Thermogravimetric Analysis

The thermal properties of the SMA copolymer and its two synthesized derivatives have been assisted by Thermogravimetric analysis. Figure. 2 illustrates the thermal behavior of the three copolymers when heated under nitrogen atmosphere with a heating rate of 10°C/min.
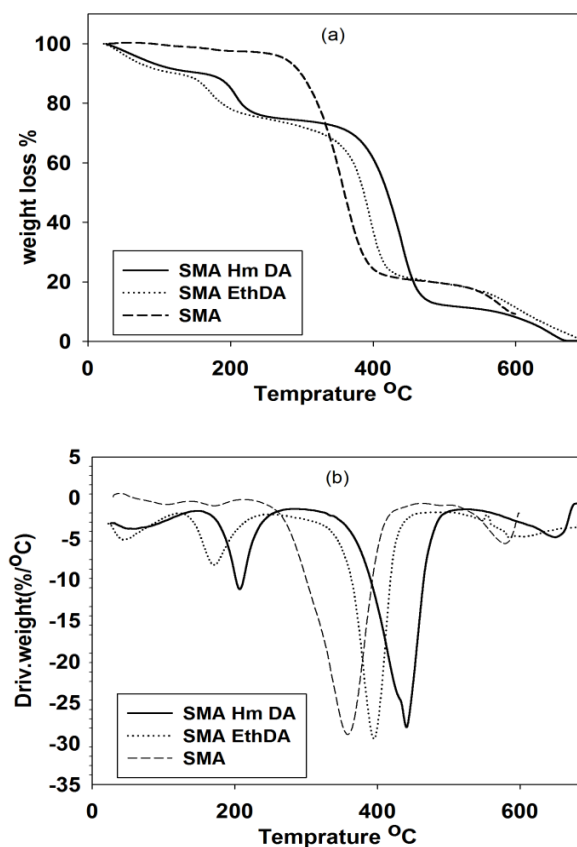

Figure 2.　Thermal analysis of SMA and derivatives

The chemical structure of the SMA backbone is significantly changed, that is, the 5-membered anhydride ring is converted either into (a) an ester carboxylic acid, (b) an ester, or (c) an imide [22]. These different chemical structures may lead to different thermos-stabilities. Figure. 2 displays the thermal behaviour of the pristine copolymer and its derivatives. The TGA reveal that the two amino derivatives are slightly more thermally stable. Figure 2b shows the first derivatives of TGA traces of SMA and SMA modified samples. As seen from the figure SMA40 copolymer decomposes in a single step at 358°C, while the modified samples exhibit two decomposition bands. For the SMA-EthDA the first decomposition step at 170°C can be attributed to the elimination of the ethylene amine side chain. The main decomposition occurs at 395°C resulting from

decomposition of the polymer backbone, which is 37°C higher than that of SMA. The first decomposition step for the SMA- HmDA is at 207°C. The main decomposition occurs at 81°C higher than that of SMA at 439°C. This behaviour indicates that the modified copolymers exhibit better thermostability than that of the original SMA copolymer.

3.2. pH Effect on the Metal Ion Adsorption

It can be seen from Figure 3 that the uptake of metal ions increases as the pH increases to reach a maximum value at around pH 4.0, 6.0 and 3.0 for Cu (II), Cd (II) and Pb (II), respectively. The number of active sites on the surface of the adsorbent may change with varying the pH. This could be explained by the fact that at low pH (acidic solution), the amine groups in the modified SMA are mostly protonated which induce an electrostatic repulsion of the metal ions [23, 24]. So, the protonation of amine groups in acidic solutions makes the polymer behaves as a cationic identity and consequently the potential for attracting metal anions decreases [25]. Therefore, competition existed between protons and metal ions for adsorption sites and consequently the adsorption capacity decreased. At higher pH values (basic solution), precipitation of metal hydroxide occurs simultaneously with the adsorption of metal ions, therefore, pH of maximum adsorption for each metal ions was chosen for further studies.
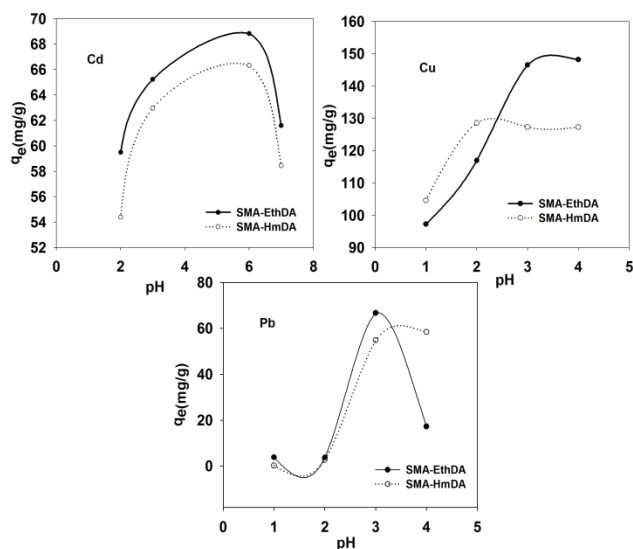

Figure 3. Effect of pH on the adsorption of Cu (II), Cd (II) and Pb (II) on modified SMA
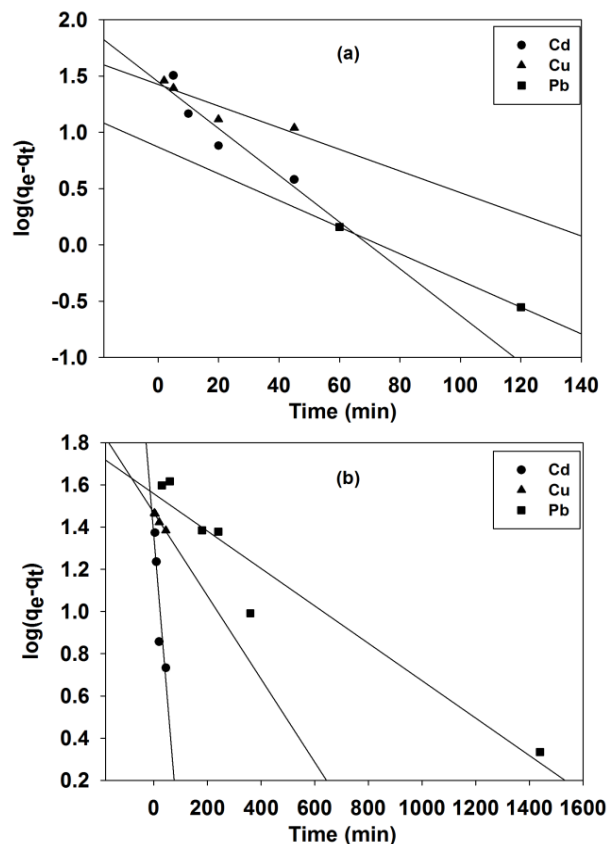
3.3. Adsorption Kinetics

From Figure 4, it can be seen that the effect of contact time on the adsorption of Cu (II) suggested that the copper adsorption is higher for the SMA-HmDA derivative than that of the SMA-EthDA derivative, which may point to an active participation of NH_2 in the process of adsorption. On the other hand, the adsorption of Cd and Pb is higher on SMA-EthDA and it takes a longer time to reach the equilibrium for these metal ion on both derivatives.

The reaction kinetic parameters for the adsorption process were studied by batch method. The pseudo-first-order [26, 27], pseudo-second-order [28, 29] and intraparticle diffusion [30] kinetic models were selected to elucidate the adsorption kinetic process in this work.
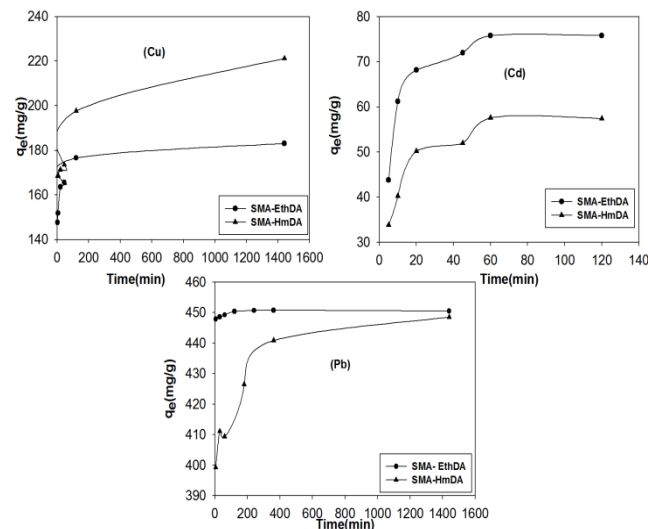
Figure 4. Effect of adsorption time on the uptake of Cd (II), Cu (II), and Pb (II) on the modified SMA
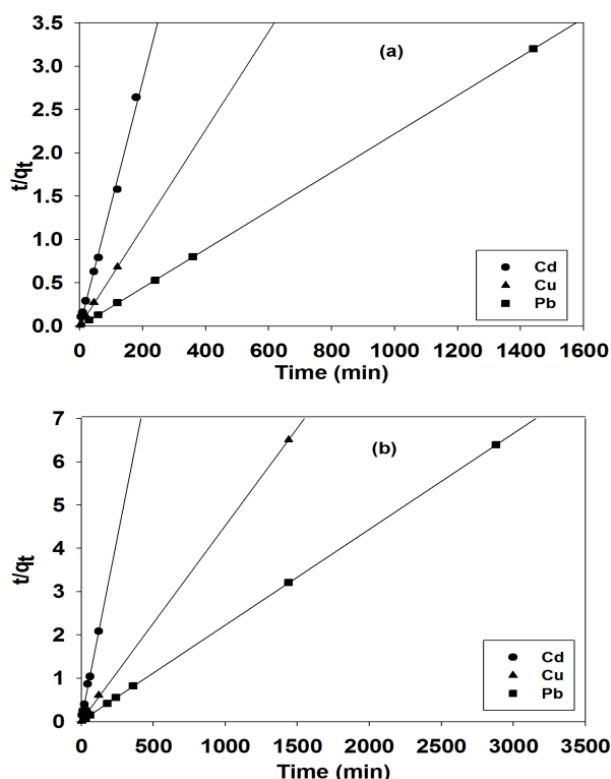

Figure 5. Pseudo-first-order kinetic plots for (a) SMA-EthDA and (b) SMA-HmDA

The Lagergren pseudo-first-order kinetic model is represented as [31, 32]:

$$\log(q_e - q_t) = \log q_e - (\frac{k_1}{2.303})t \qquad (3)$$

Where k_1 is the pseudo-first-order rate constant (min^{-1}) of adsorption, q_e and q_t (mg/g) are the amounts of metal ion adsorbed at equilibrium and at time t (min), respectively. The q_e and rate constant k_1 were calculated by plotting the log $(q_e - q_t)$ versus t. The plots for pseudo-first-order model are presented in Figure. (5).

$$\frac{t}{q_t} = \frac{1}{k_2 q_e^2} + (\frac{1}{q_e})t \qquad (4)$$

Where k_2 is the pseudo-second-order rate constant of adsorption (g mg^{-1} min^{-1}). The kinetic parameters for pseudo-second-order model are determined from the linear plots of (t/q_t) versus t. The plots for pseudo-second-order model are presented in Figure. (6).

The parameters for pseudo-first and pseudo-second order models are all shown in (Table 2).

As shown in Table (2), according to the correlation coefficients (R^2), the calculated q_e value of pseudo-second-order kinetic model is in good agreement with the experimental q_e value and could better fit the adsorption of metal ion on the resin very well. The adsorbent systems can be well-described by the pseudo second-order kinetic model. The phenomenon also implies that the chelating reaction is the main adsorption mechanism of the adsorption process [33].

The initial adsorption rate (h) can be determined from k_2 and q_e values using

$$h = k_2 q_e^2 \qquad (5)$$

The intra-particle diffusion model was used to test whether the adsorption rate is controlled by the diffusion mechanism.

The linear form intra-particle diffusion kinetic model based on the theory or equation proposed by Weber and Morris is tested [21, 34]. The adsorbate uptake varies almost proportionally with $t_{1/2}$ according to the following Weber–Morris's equation:

$$q_t = k_{id} t^{1/2} + C \qquad (6)$$

Where k_{id} is the rate parameter of stage i (mg/g h$^{1/2}$), calculated from the slope of the straight line of qt versus $t^{1/2}$. C_i is the intercept of stage i, giving an idea about the thickness of boundary layer. That is to say, the larger the intercept indicates the greater the boundary layer effect.

Figure 6. Pseudo-second-order kinetic plots for a) SMA-EthDA and (b) SMA-HmDA

The pseudo-second order model can be written as [21]:

Table 2. Parameters for pseudo-first and pseudo-second order

Metal ions		Pseudo first order		Pseudo Second order			Intraparticle diffusion
		K_1 (min^{-1})	R_2	q_e	K_2 (gmg^{-1}min^{-1})	R_2	K_{int}
Cd	SMA-EthDA	4.250	-0.0461	0.87	70.496	-0.034	0.990	9.600
	SMA-HmDA	3.857	-0.034	0.81	59.662	0.004	0.990	7.110
Cu	SMA-EthDA	3.974	-1.37E-02	0.65	162.608	-0.016	0.990	27.68
	SMA-HmDA	4.340	-4.54E-03	0.98	197.863	0.002	0.990	24.53
Pb	SMA-EthDA	1.768	-2.04E-02	0.96	450.754	0. 015	0.990	32.59
	SMA-HmDA	5.528	-4.18E-03	0.94	450.7538	0.015	0.990	36.21

Figure. 7 represents a linear fit of intra-particle diffusion model for adsorption of heavy metal ions onto SMA modified copolymer. The multi-linearity plot indicates three steps of diffusion.
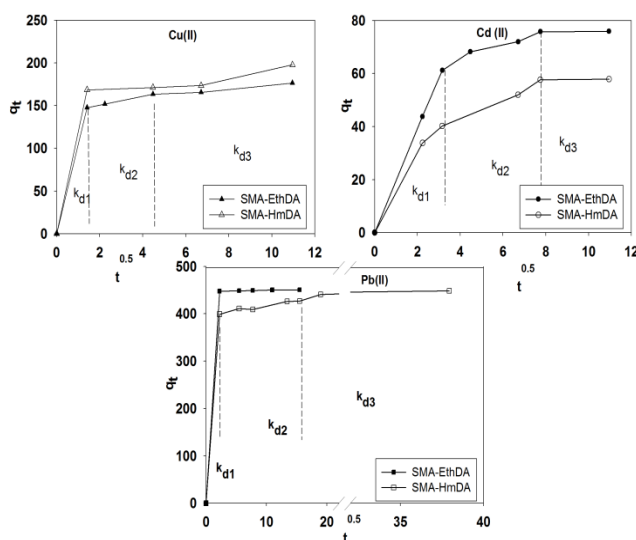

Figure 7.   Plots for intra-particle diffusion

First, the metal ions were rapidly transported from solution, due to the high initial heavy metal ion concentration and the availability of adsorbing sites on the surfaces of modified SMA. The sharpness of this region is often assumed to be attributed to the high diffusion of adsorbate through the solution to the external surface of adsorbent [35].

Then this step is followed by a much slower region II. At this stage, the diffusion resistance increases [36] and consequently the adsorption decrease leading to a lower and lower diffusion rate. The third region is the final equilibrium stage where intra-particle diffusion further slows down because of the low concentrations of heavy metal ions left in the solutions [37]. Table (3) lists values of k_{d1} k_{d2} and k_{d3} for adsorption of Cd (II), Cu (II) and Pb (II) by modified SMA. As expected, it was found that $k_{d1} > k_{d2}$ for all metal ions.

The rate of external surface adsorption (the first region) of Pb(II) is higher than that the other ions with SMA-EthDA and SMA-HmDA because Pb (II)ion has the strongest binding affinity with ligand and the smallest hydrated ionic radius, which lead to the highest priority to be absorbed.

3.4. Adsorption Isotherms*

Isotherm data were applied to two adsorption models and the results of their linear regression were used to find out the model which best fit the obtained data. Values of the resulting parameters and the regression coefficients (R_2) are listed in Table 4.

Table 3.   Intra-particle diffusion model constants and correlation coefficients for adsorption of metal ions on modified SMA

Metal Ions		Intra-particle diffusion model								
		K_{d1} (mg/g min$^{1/2}$)	K_{d2} (mg/g min$^{1/2}$)	K_{d3} (mg/g min$^{1/2}$)	C_1	C_2	C_3	$(R_1)^2$	$(R_2)^2$	$(R_3)^2$
Cd	SMA-EthDA	19.58	2.91	0.03	0	53.21	75.74	1	0.94	0.99
	SMA-HmDA	15.11	3.86	0.09	0	26.40	56.87	1	0.98	1
Cu	SMA-EthDA	104.45	5.19	2.59	0	140.31	148.22	1	0.99	1
	SMA-HmDA	119.07	0.98	5.68	0	166.80	135.35	1	0.97	1
Pb	SMA-EthDA	200.27	0.25	0.02	0	447.24	450.30	1	0.99	1
	SMA-HmDA	178.56	0.96	0.13	0	167.01	443.29	1	0.99	1

Table 4.   Isotherm model parameters for the adsorption of metal ion on the modified SMA

Metal ion		Langmuir				Freundlich		
		Q_{max} (mg g^{-1})	K_L (Lmg^{-1})	R_2	R_L	n	K_F	R_2
Cd	SMA-EthDA	0.14	0.519	0.98	0.0017	5	1.54	0.90
	SMA-HmDA	0.20	4.383	0.95	0.0002	2.38	9.874	0.95
Cu	SMA-EthDA	100	0.038	0.94	0.034	1.89	1.69	0.89
	SMA-HmDA	100	0.003	0.94	0.260	4.35	18.54	0.92
Pb	SMA-EthDA	3.33	0.0002	0.99	0.928	-0.4	26.84	0.89
	SMA-HmDA	10	-0.002	0.99	-0.878	-0.4	108.85	0.90

The Langmuir isotherm model is derived to model the assumptions of monolayer adsorption, a certain number of identical active sites, active sites distributed evenly on the surface of the adsorbent, and no interaction between adsorbents [38]. The equation for the Langmuir isotherm is as follows:

$$\frac{C_e}{q_e} = \frac{C_e}{Q_{max}} + \frac{1}{K_L Q_{max}} \qquad (7)$$

where C_e is the equilibrium concentration of metal ions in solution (mg/l), qe the adsorbed value of metal ions at equilibrium concentration (mmol/g), Q_{max} (mg/g) and K_L (l/mg) are the Langmuir constants which are related to maximum adsorption capacity of adsorbents (mg g^{-1}) and energy of adsorption (mg L^{-1}), respectively, and can be calculated from the intercept and slope of the linear plot, with C_e/q_e versus C_e.

The essential characteristics of the Langmuir equation can be expressed in term of a dimensionless separation factor, RL defined as follows [39–41]

$$R_L = \frac{1}{1+K_L C_0} \qquad (8)$$

Where C_o is the highest initial solute concentration, and K_L is the Langmuir's adsorption constant (L/mg). From Table (4), it can be found the values of R_L were in the range of 0–1, confirming the favorable uptake of these heavy metal ions.

The Freundlich isotherm is proposed based on multilayer adsorption and adsorption on heterogeneous surfaces, which can be illustrated as [42]:

$$q_e = K_F \, C_e^{1/n} \qquad (9)$$

Where q_e and C_e are equilibrium concentration of metal ion in adsorbent (mg/g) and liquid phase (mg/l), respectively. K_F and n are the Freundlich constants. The linearized equation takes the form:

$$\ln q_e = \frac{1}{n} \ln C_e + \ln K_F \qquad (10)$$

Where K_F and n are the Freundlich constants, which related to adsorption capacity of adsorbent and the adsorption strength, respectively. K_F and n can be obtained from the intercept and the slope of the linear plot of ln q_e versus ln C_e.

The Freundlich model assumes heterogeneous adsorption due to the diversity of the adsorption sites or the diverse nature of the metal ions adsorbed, free or hydrolyzed species [40].

Table 4 displays the coefficients of the Langmuir and Freundlich models along with regression coefficients (R_2).

As seen from Figure.8 and 9. , the R_2 values were above 0.90 for both the Langmuir and Freundlich isotherm models, suggesting that both models closely fit the experimental results. However, the R_2 values indicate that the Langmuir isotherm fit the experimental data better than the Freundlich

at room temperature. The maximum adsorption capacity of the monolayer (Q_m) values for Cu(II) was higher than those of Cd (II) and Pb (II), showing the following order: Cu (II) > Pb (II) > Cd (II).
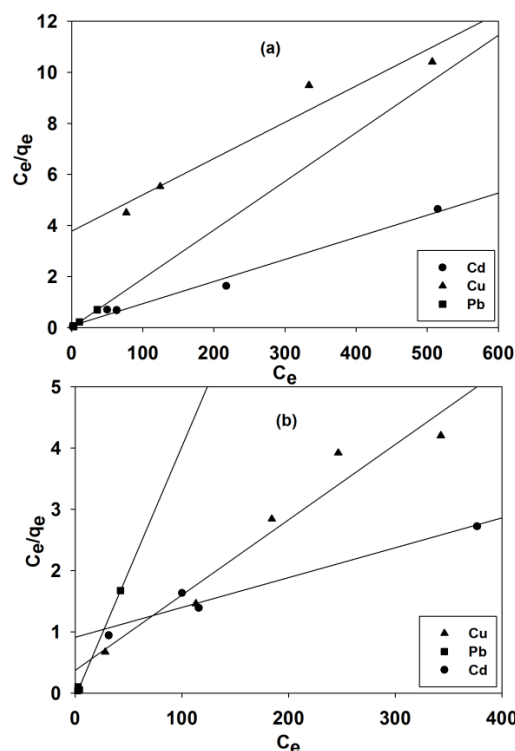
Figure 8. Langmuir adsorption isotherm for (a) SMA-EthDA and (b) SMA-HmDA
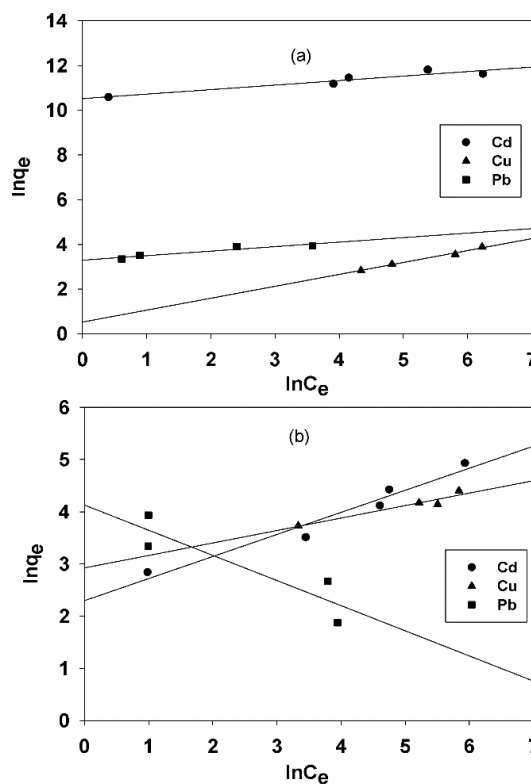
Figure 9. Adsorption isotherm for (a) SMA-EthDA and (b) SMA-HmDA

3.5. X-ray Diffraction

The degree of crystallinity of the samples was determined by the known procedures [43, 44]. The structural properties of modified SMA and the adsorbed metal ion were studied in the range 2 Θ = 40-90°

The degree of crystallinity, χ_{cr}, is frequently determined from the ratio of the integral intensity of the peak of the crystalline regions in the diffraction pattern to the total integral peak. To calculate the intensity of the peak originating from the crystalline regions in the samples, the total area under the diffraction curve S_{tot} and the area of the amorphous component Sam were determined graphically.

The degree of crystallinity, χ_{cr}, was calculated by the following expression:

$$X_{cr} = \frac{S_{tot} - S_{am}}{S_{tot}} x(100) \qquad (10)$$

Where S_{tot} is the total area under the diffraction curve in the angle range 4°-90° and Sam, the area of the amorphous component in the same range. The degrees of crystallinity evaluated by the above procedure are shown in Figure10 and listed in the table (5). The main peak in the XRD pattern of SMA is observed at 2 Θ = 19.97°. In the case of this peak is shifted to 2 Θ = 22.48° and 22.59° for SMA-EthDA and SMA-HmDA, respectively.
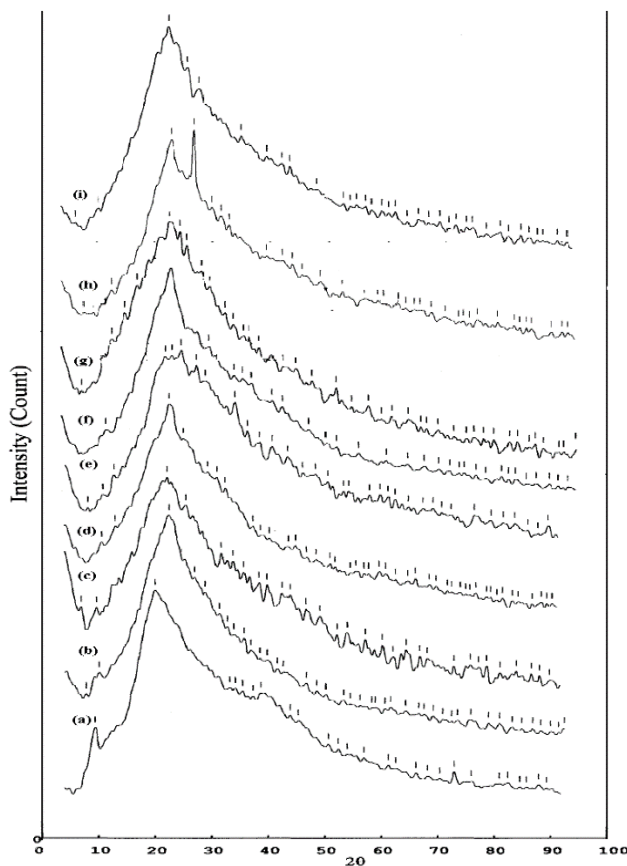
Figure 10. (a) SMA (b)SMA-EthDA(c) SMA-EthDA-Cd (d) SMA-EthDA-Cu (e) SMA-EthDA-Pb (f)SMA-HmDA(g) SMA-HmDA-Cd (h) SMA-HmDA-Cu (i) SMA-HmDA-Pb

Table 5. Crystallinity percentage of the prepared polymers with and without metals

Sample	The degree of crystallinity%	d (A°)
SMA	54.69	4.44
SMA - EthDA	63.83	8.72
SMA - Eth DA-Cd	70.55	4.02
SMA - EthDA-Cu	64.91	3.54
SMA - EthDA-Pb	74.88	3.62
SMA - HmDA	70.09	3.92
SMA - HmDA-Cd	76.88	3.64
SMA - HmDA-Cu	75.53	3.30
SMA - HmDA-Pb	75.71	3.94

It should be noted that the weak peaks observed in the XRD patterns of the SMA are absent in the XRD patterns of SMA-EthDA and SMA-HmDA. The incorporation of metal ion increases the degrees of crystallinity Pb(II)> Cd(II) >Cu(II).

4. Conclusions

The modified styrene-co-maleic copolymer have been successfully prepared by the reaction of two different alkyl diamine with SMA copolymer, and was used for the adsorption of Cd (II), Cu (II) and Pb (II) from aqueous solutions. The results suggest that the adsorption is influenced by solution pH, initial concentration of the metal ions and contact time. The experimental data were well fitted by the Langmuir isotherm model and the adsorption coefficients agreed well with the conditions supporting favorable adsorption.

The adsorption kinetics was found to fit the pseudo second- order kinetics very well with rapid initial sorption rate. The reaction of the SMA copolymer with diamines leads to more thermally stable products.

REFERENCES

[1]   Nwuche, C.O., and Ugoji, E.O., 2008, Effects of heavy metal pollution on the soil microbial activity, Int. J. Environ. Sci. Technol. 5(3), 409–414.

[2]   Sternberg, S.P.K., and Dorn, R.W., 2002, Cadmium removal using Cladophora in batch, semi-batch and flow reactors, Bioresource Technology 81(3), 249–255.

[3]   Liang, X., Su, Y., Yang, Y., and Qin, W., 2012, Separation and recovery of lead from a low concentration solution of lead (II) and zinc (II) using the hydrolysis production of poly styrene-co-maleic anhydride, Journal of hazardous materials 203, 183–187.

[4]   Bowen, Humphry John Moule, Environmental chemistry of the elements, Academic Press, 1979.

[5]   Yu, B., Zhang, Y., Shukla, A., Shukla, S.S., and Dorris, K.L.,

2001, The removal of heavy metals from aqueous solutions by sawdust adsorption—removal of lead and comparison of its adsorption with copper, Journal of hazardous materials 84(1), 83–94.

[6] Leyva-Ramos, R., Rangel-Mendez JR, Mendoza-Barron, J., Fuentes-Rubio, L., and Guerrero-Coronado, R.M., 1997, Adsorption of cadmium (II) from aqueous solution onto activated carbon, Water Science and Technology 35(7), 205–211.

[7] Emongor, V., 2007, Biosorption of lead from aqueous solutions of varied pH by kale plants (Brasicca oleraceae varacephala), Journal of Agricultural, Food and Environmental Sciences 1(2), 90–91.

[8] Madadrang, C.J., Kim, H.Y., Gao, G., Wang, N., Zhu, J., Feng, H., Gorring, M., Kasner, M.L., Hou, S.F, 2012, Adsorption behavior of EDTA-graphene oxide for Pb (II) removal, ACS Appl. Mater. Interfaces 4, 1186–1193.

[9] Liu, D.G., Li, Z.H., Li, W., Zhong, Z.R., Xu, J.Q. J.J. Ren, Z.S. Ma, 2013, Adsorption behavior of heavy metal ions from aqueous solution by soy protein hollow microspheres, Ind. Eng. Chem. Res. 52, 11036–11044.

[10] Zhao, G., Wu, X., Tan, X., and Wang, X., 2011, Sorption of heavy metal ions from aqueous solutions: a review, Open Colloid Science Journal 4, 19–31.

[11] Chen, J. H., Hsu, K.C., Chang, Y. M., 2013, Surface modification of hydrophobic resinwith tricaprylmethylammonium chloride for the removal of trace hexavalent chromium, Ind. Eng. Chem. Res. 52 (2013) 11685–11694

[12] Othman, M.K., Al-Qadri, F.A., and Al-Yusufy, F.A., 2011, Synthesis, physical studies and uptake behavior of: Copper (II) and lead (II) by Schiff base chelating resins, Spectrochimica Acta Part A: Molecular and Biomolecular Spectroscopy 78(5), 1342–1348.

[13] Wang, Y.P., Shen, Y.Q., Pei, X.W., Zhang, S.C., Liu, H.G., Ren, J.M., In situ synthesis of poly(styrene-co-maleic anhydride)/SiO2 hybrid composites via 'grafting onto'strategy based on nitroxide-mediated radical polymerization, React. Funct. Polym. 68 (2008) 1225–1230.

[14] Krüger, S., Krahl, F., Arndt, K.F., 2010, Random cross-linked poly(styrene-co-maleicanhydride): characterization of cross-linking intermediates by size exclusion chromatography, Eur. Polym. J. 46, 1040–1048.

[15] Qi, X.-H., Jia, X.-Q., Ying, Y., Niu, L.-E., and Hou, L.-P., 2010, Recovery of nickel from mixed solution containing light metals by PSt/MA resin, Transactions of Nonferrous Metals Society of China 20, s102.

[16] McClain, A.R., and Hsieh, Y.-L., 2004, Synthesis and metal complexation of dihydroxyphosphino-functionalized crosslinked styrene/maleic anhydride copolymers, J. Polym. Sci. A Polym. Chem. 42(1), 92–101.

[17] Lin, J.-J., and Hsu, Y.-C., 2009, Temperature and pH-responsive properties of poly (styrene-co-maleic anhydride)-grafting poly (oxypropylene)-amines, Journal of colloid and interface science 336(1), 82–89.

[18] Gonte, R.R., and Balasubramanian, K., 2012, Chemically modified polymer beads for sorption of gold from waste gold solution, Journal of hazardous materials 217, 447–451.

[19] Zhu, Z., Sun, F., Yang, L., Gu, K., Li, W., 2013, Poly (styrene-co-maleic anhydride) microspheres prepared in ethanol/ water using a photochemical method and their application in Ni^{2+}adsorption, Chemical Engineering Journal 223, 395–401.

[20] Wei, K., Wu, J., Chen, Y., Hsu, Y., and Lin, J., 2007, Easy preparation of crosslinked polymer films from polyoxyalkylene diamine and poly (styrene–maleic anhydride) for electrostatic dissipation, Journal of applied polymer science 103(2), 716–723.

[21] Ma, X., Li, L., Yang, L., Su, C., Wang, K., Yuan, S., and Zhou, J., 2012, Adsorption of heavy metal ions using hierarchical $CaCO_3$–maltose meso/macroporous hybrid materials: Adsorption isotherms and kinetic studies, Journal of hazardous materials 209, 467–477.

[22] Bruch, M., Mäder, D., Bauers, F., Loontjens, T., and Mülhaupt, R., 2000, Melt modification of poly (styrene‐co‐maleic anhydride) with alcohols in the presence of 1, 3‐oxazolines, Journal of Polymer Science Part A: Polymer Chemistry 38(8), 1222–1231.

[23] Haider, S., and Park, S.-Y., 2009, Preparation of the electrospun chitosan nanofibers and their applications to the adsorption of Cu (II) and Pb (II) ions from an aqueous solution, Journal of Membrane Science 328(1), 90–96.

[24] Ngah, W.W., Endud, C.S., and Mayanar, R., 2002, Removal of copper (II) ions from aqueous solution onto chitosan and cross-linked chitosan beads, Reactive and Functional Polymers 50(2), 181–190.

[25] Guibal, E., Ruiz, M., Vincent, T., Sastre, A., and Navarro-Mendoza, R., 2001, Platinum and palladium sorption on chitosan derivatives, Separation Science and Technology 36(5-6), 1017–1040.

[26] Justi, K.C., Fávere, V.T., Laranjeira, M.C.M., Neves, A., and Peralta, R.A., 2005, Kinetics and equilibrium adsorption of Cu (II), Cd (II), and Ni (II) ions by chitosan functionalized with 2 [-bis-(pyridylmethyl) aminomethyl]-4-methyl-6-form ylphenol, Journal of colloid and interface science 291(2), 369–374.

[27] Wang, L., Xing, R., Liu, S., Yu, H., Qin, Y., Li, K., Feng, J., Li, R., and Li, P., 2010, Recovery of silver (I) using a thiourea-modified chitosan resin, Journal of hazardous materials 180(1), 577–582.

[28] Ho, Y.-S., 2006, Second-order kinetic model for the sorption of cadmium onto tree fern: a comparison of linear and non-linear methods, Water research 40(1), 119–125.

[29] Ho, Y.-S., and McKay, G., 2000, The kinetics of sorption of divalent metal ions onto sphagnum moss peat, Water research 34(3), 735–742.

[30] Weber, W.J., and Morris, J.C., 1963, Kinetics of adsorption on carbon from solution, Journal of the Sanitary Engineering Division 89(2), 31–60.

[31] Wang, P., Du, M., Zhu, H., Bao, S., Yang, T., and Zou, M., 2015, Structure regulation of silica nanotubes and their adsorption behaviors for heavy metal ions: pH effect, kinetics, isotherms and mechanism, Journal of hazardous materials 286, 533–544.

[32] Donia, A.M., Atia, A.A., and Elwakeel, K.Z., 2008, Selective

separation of mercury (II) using magnetic chitosan resin modified with Schiff's base derived from thiourea and glutaraldehyde, Journal of hazardous materials 151(2), 372–379.

[33] Hua, M., Jiang, Y., Wu, B., Pan, B., Zhao, X., and Zhang, Q., 2013, Fabrication of a new hydrous Zr (IV) oxide-based nanocomposite for enhanced Pb (II) and Cd (II) removal from waters, ACS applied materials & interfaces 5(22), 12135–12142.

[34] Weber, W.J., and Morris, J.C., 1962, Proceeding of the International Conference on Water Pollution Symposium, Pergamon Press, Oxford 2, 235–266.

[35] Sadeghi, S., Rad, F.A., and Moghaddam, A.Z., 2014, A highly selective sorbent for removal of Cr (VI) from aqueous solutions based on Fe 3 O 4/poly (methyl methacrylate) grafted Tragacanth gum nanocomposite: Optimization by experimental design, Materials Science and Engineering: C 45, 136–145.

[36] Mututuvari, T.M., and Tran, C.D., 2014, Synergistic adsorption of heavy metal ions and organic pollutants by supramolecular polysaccharide composite materials from cellulose, chitosan and crown ether, Journal of hazardous materials 264, 449–459.

[37] Tan, I.A., Ahmad, A.L., and Hameed, B.H., 2009, Adsorption isotherms, kinetics, thermodynamics and desorption studies of 2, 4, 6-trichlorophenol on oil palm empty fruit bunch-based activated carbon, Journal of hazardous materials 164(2), 473–482.

[38] Wang, J., Zhou, Y., Li, A., and Xu, L., 2010, Adsorption of humic acid by bi-functional resin JN-10 and the effect of alkali-earth metal ions on the adsorption, Journal of hazardous materials 176(1), 1018–1026.

[39] Ramesh, A., Hasegawa, H., Sugimoto, W., Maki, T., and Ueda, K., 2008, Adsorption of gold (III), platinum (IV) and palladium (II) onto glycine modified crosslinked chitosan resin, Bioresource Technology 99(9), 3801–3809.

[40] Wang, X., Zhang, Y., and Li, Q., 2011, Characterization and determination of the thermodynamic and kinetic properties of the adsorption of molybdenum (VI) onto microcrystalline anthracene modified with 8-hydroxyquinoline, Materials Science and Engineering: C 31(8), 1826–1831.

[41] Hall, K.R., Eagleton, L.C., Acrivos, A., and Vermeulen, T., 1966, Pore-and solid-diffusion kinetics in fixed-bed adsorption under constant-pattern conditions, Industrial & Engineering Chemistry Fundamentals 5(2), 212–223.

[42] Jin, X., Li, Y., Yu, C., Ma, Y., Yang, L., and Hu, H., 2011, Synthesis of novel inorganic–organic hybrid materials for simultaneous adsorption of metal ions and organic molecules in aqueous solution, Journal of hazardous materials 198, 247–256.

[43] Chebotok, E.N., Novikov, V.Y., and Konovalova, I.N., 2007, Kinetics of base deacetylation of chitin and chitosan as influenced by their crystallinity, Russian Journal of Applied Chemistry 80(10), 1753–1758.

[44] I. Boucher, K. Jamieson, A. Retnakaran, Advances in Chitin Science, Vol7.(Montreal: 9th ICCC), 2004.